Structure and Magnetic Properties of Trigonal Bipyramidal Iron Nitrosyl Complexes

Manabendra Ray,[†] Adina P. Golombek,[‡] Michael P. Hendrich,*[,‡] Glenn P. A. Yap,[§] Louise M. Liable-Sands,[§] Arnold, L. Rheingold,[§] and A. S. Borovik*[,†]

Departments of Chemistry, University of Kansas, Lawrence, Kansas 66045, Carnegie-Mellon University, Pittsburgh, Pennsylvania 15213, and University of Delaware, Newark, Delaware 19716

Received January 12, 1999

Non-heme Fe(II) proteins form stable nitrosyl adducts. However, there are few synthetic examples of structurally characterized non-heme iron nitrosyl complexes, especially those that are coordinatively unsaturated. Presented herein is a series of non-heme $\{Fe-NO\}^7$ complexes with trigonal bipyramidal coordination geometry. These complexes were synthesized with tripodal ligands derived from tris(*N*-R-carbamoylmethy)amine $[\mathbf{1}^R]^{3-}$ where R = isopropyl (^{i}Pr), cyclopentyl (cyp), or 3,5-dimethylphenyl (dmp) groups. The R groups of these $[\mathbf{1}^R]^{3-}$ ligands form cavities around the metal ion that can influence structural and functional properties. The nitrosyl complexes were synthesized by treating the Fe(II) precursors $[Fe\mathbf{1}^R]^-$ with NO at room temperature. These iron nitrosyl complexes have similar molecular structures as determined by X-ray diffraction methods. They differ in their Fe−N−O angles which range from 178.2(5)° in $[Fe\mathbf{1}^i Pr(NO)]^-$ to 160.3(2)° in $[Fe\mathbf{1}^{dmp}(NO)]^-$. The observed difference in angle is related to the cavity size: $[Fe\mathbf{1}^i Pr(NO)]^-$ has the most restricted cavity with a small diameter ($\sim$ 3 Å) while $[Fe\mathbf{1}^{dmp}(NO)]^-$ is more flexible and larger ($\sim$8 Å diameter). This angular difference is supported by EPR measurements which shows that $[Fe\mathbf{1}^{dmp}(NO)]^-$ has a significantly more rhombic spectrum than that found for $[Fe\mathbf{1}^i Pr(NO)]^-$. Magnetic moment, Mössbauer and EPR data on these $\{Fe-NO\}^7$ complexes agree with a electronic configuration of [Fe^{3+} d^5 HS ($S = {}^5/_2$)−NO^- ($S = 1$)] that lead to an $S = {}^3/_2$ ground state via antiferromagnetic coupling.

Introduction

Nitric oxide has been shown to bind to the Fe(II) state of many mononuclear non-heme iron enzymes. Examples include soybean lipoxygenase,[1] protocatechuate 4,5-dioxygenase,[2] catecholate 2,3-dioxygenase,[3] putidamonooxin,[4] and isopenicillin N synthase.[5] Many of these Fe−NO adducts have stable $S = {}^3/_2$ ground states and serve as analogues for the possible dioxygen intermediates involved in catalysis. Surprisingly, there are few synthetic examples of structurally characterized non-heme $\{Fe-NO\}^7$ complexes with $S = {}^3/_2$ spin states that can be used as models for these protein derivatives.[6−8] Most previously published non-heme$\{Fe-NO\}^7$ complexes are six-coordinate having Fe−N−O bond angles <160°.[9] We have reported recently the first example of a trigonal bipyramidal $\{Fe-NO\}^7$ complex $[Fe\mathbf{1}^{S\text{-mbz}}(NO)]^-$,[10] using a chiral tripodal ligand which is derived from tris(*N*-R-carbamoylmethy)amine $[\mathbf{1}^R]^{3-}$.

This class of tripodal ligands, when bonded to a metal ion, forms cavities around vacant coordination sites on metal ions.[11] Our initial structural study with $[Fe\mathbf{1}^{S\text{-mbz}}(NO)]^-$ revealed a relationship between cavity structure and the angle of the Fe−NO unit: cavities that had relatively small size supported nearly linear Fe−N−O motifs while those having larger cavities yield nonlinear Fe−N−O units. To further probe this structural relationship we have synthesized $[Fe\mathbf{1}^R(NO)]^-$ complexes where R = isopropyl, cyclopentyl, and 3,5-dimethylphenyl. This report describes the structural and physical properties of these trigonal bipyramidal $\{Fe-NO\}^7$ complexes and substantiates the correlation between cavity structure and Fe−N−O bond angle noted in our earlier work.[10] Moreover, magnetic studies indicate

[†] University of Kansas.
[‡] Carnegie-Mellon University.
[§] University of Delaware.

(1) Nelson, M. J. *J. Biol. Chem.* **1987**, *262*, 12137.
(2) Arciero, D. M.; Lipscomb, J. D. *J. Biol. Chem.* **1986**, *261*, 2170.
(3) Arciero, D. M.; Oriville, A. M.; Lipscomb, J. D. *J. Biol. Chem.* **1985**, *260*, 14035.
(4) Twilfer, H.; Bernhardt, F.-H.; Gersonde, K. *Eur. J. Biochem.* **1985**, *147*, 171.
(5) Chen, V. J.; Orville, A. M.; Harpel, M. R.; Frolik, C. A.; Surerus, K. K.; Münck, E.; Lipscomb, J. D. *J. Biol. Chem.* **1989**, *264*, 21677.
(6) (a) Hodges, K. D.; Wollmann, R. G.; Kessel, S. L.; Hendrickson, D. N.; Van Derveer, D. G.; Barefield, K. E. *J. Am. Chem. Soc.* **1979**, *101*, 906. (b) Haller, K. J.; Johnson, P. L.; Feltham, R. D.; Enemark, J. H.; Ferrara, J. R.; Basile, L. T. *Inorg. Chim. Acta* **1979**, *33*, 119. (c) Pohl, K.; Wiegardht, K.; Nuber, B.; Weiss, J. *J. Chem. Soc., Dalton Trans.* **1987**, 187. (d) Randall, C. R.; Zang, Y.; True, A. E.; Que, L., Jr.; Charnock, J. M.; Garner, C. D.; Fujishima, Y.; Schofield, C. J.; Baldwin, J. E. *Biochemistry*, **1993**, *32*, 6664. (e) Westre, T. M.; Di Cicco, A.; Filiponi, A.; Natoli, C. R.; Hedman, B.; Solomon, E. I.; Hodgson, K. O. *J. Am. Chem. Soc.* **1994**, *116*, 6757. (f) Chiou, Y.-M.; Que, L., Jr. *Inorg. Chem.* **1995**, *34*, 3270.
(7) Reviews: (a) Enemark, J. H.; Feltham, R. D. *Coord. Chem. Rev.* **1974**, *13*, 339. (b) Feltham, R. D.; Enemark, J. H. *Top. Stereochemistry* **1981**, *12*, 155. (c) Richter-Addo, G. B.; Legzdins, P. *Metal Nitrosyls*; Oxford University Press: New York, 1992.
(8) The Enemark−Feltham nomenclature for $\{MNO\}^x$ is used where *x* is the number of d electrons in the system when the nitrosyl ligand is formally considered NO^+.
(9) The only square planar or six-coordinate non-heme $\{Fe-NO\}^7$ complex with an Fe−N−O angle >175° is $[Fe(TMC)(NO)](BF_4)_2$ where TMC is 1,4,8,11-tetramethyl-1,4,8,11-tetraazacyclotetradecane1.[6a]
(10) Hammes, B. S.; Maldonado-Ramos, D.; Yap, G. P. A.; Liable-Sands, L.; Rheingold, A. L.; Borovik, A. S. *Inorg. Chem.* **1997**, *36*, 3210.
(11) (a) Ray, M.; Yap, G. P. A.; Rheingold, A., Borovik, A. S. *J. C. S., Chem. Commun*. **1995**, 1777. (b) Ray, M.; Golombek, A.; Hendrich, M.; Young, V. G., Jr.; Borovik, A. S. *J. Am. Chem. Soc.* **1996**, *118*, 6084. (c) Shirin, Z.; Young, V. G., Jr.; Borovik, A. S. *Chem. Commun.* **1997**, *4*, 1840. (d) Ray, M.; Hammes, B. S.; Yap, G. P. A.; Rheingold, Liable-Sands, L.; Borovik, A. S. *Inorg. Chem.* **1998**, *37*, 1527. (e) Hammes, B. S.; Ramos-Maldonado, D.; Yap, G. P. A.; Rheingold, A. L.; Young, V. G, Jr.; Borovik, A. S. *Coord. Chem. Rev.* **1998**, *174*, 241.

10.1021/ic990070a CCC: $18.00
Published on Web 05/29/1999

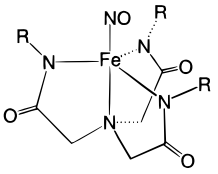

Complex	R
$[Fe\mathbf{1}^{S\text{-}mbz}(NO)]^{1-}$	*N*-(*S*)-(-)-(α)-methylbenzyl
$[Fe\mathbf{1}^{iPr}(NO)]^{1-}$	isopropyl
$[Fe\mathbf{1}^{cyp}(NO)]^{1-}$	cyclopentyl
$[Fe\mathbf{1}^{dmp}(NO)]^{1-}$	3,5-dimethylphenyl

that the $S = {}^3/_2$ ground state observed for these {Fe−NO}^{7} complexes arises from the antiferromagnetic coupling between high spin ferric ions ($S = {}^5/_2$) and the coordinated NO^- ($S = 1$) ligands.

Experimental Section

All reagents and solvents were purchased from commercial sources and used as received unless otherwise noted. Solvents were deaerated by bubbling Ar for 30 min. The ligands $H_3\mathbf{1}^{i}Pr$ and $H_3\mathbf{1}^{cyp}$ were synthesized by procedures reported previously.[11] All manipulations involving metal complexes were done under an Ar atmosphere using a Vacuum Atmospheres drybox.

Tris(*N*-(3,5 dimethylphenyl)carbamoylmethyl)amine ($H_3\mathbf{1}^{dmp}$). 3,5-Dimethyl aniline (15.1 g, 157 mmol) was added slowly to a slurry of nitrilotriacetic acid (10.0 g, 52.3 mmol) in 40 mL of pyridine and stirred for 1 h. After the mixture was heated to 80 °C, triphenyl phosphite (49.0 g, 158 mmol) was added dropwise. The reaction mixture was stirred at 90 °C for 12 h. After the reaction had cooled to room temperature, 150 mL of diethyl ether was added and the mixture was stirred for 1 h. This mixture was filtered and the resultant solid was washed three time with chloroform and twice with diethyl ether to yield $H_3\mathbf{1}^{dmp}$ (15.0 g, 58%) as a white solid. ^{1}H NMR (DMSO-d_6) δ 2.22 (s, 18 H, $-CH_3$), 3.61 (s, 6 H, $-CH_2$-), 6.70 (s, 3 H, *p*-C_6H_6), 7.27 (s, 6 H, *o*-C_6H_6), 10.15 (s, 3 H, N*H*); MH^+ *m*/*e* 501 (+ FAB in TG/G, DMSO); FTIR (Nujol, cm^{-1}), ν(NH) 3295 (s), 3238 (sh), 3184 (s), 3153 (s), 3063 (s); ν(CO) 1686 (s), 1672 (s); mp 233 °C (dec).

Potassium [(Tris(*N*-cyclopentylcarbamoylmethyl)aminato)(nitroso)]ferrate(III) K[Fe1^{cyp}(NO)]·DMF). The ligand $H_3\mathbf{1}^{cyp}$ (0.200 g, 0.510 mmol) was deprotonated with KH (0.062 g, 1.53 mmol) in 10 mL of DMF. After H_2 evolution ceased, solid $Fe(OAc)_2$ (0.089 g, 0.51 mmol) was added in one portion and the mixture was stirred for 2 h. After being filtered to remove the insoluble KOAc, the yellow filtrate was transferred to a Schlenk tube and NO (15 mL, 0.668 mmol) was added using a gastight syringe. The addition of NO changed the color of the solution to dark red. A 40 mL amount of diethyl ether was added to this solution, and red crystals (0.13 g, 44%) were obtained after 24 h. These crystals were washed with diethyl ether and dried under vacuum. X-ray-quality crystals were grown by diffusing diethyl ether into a DMF solution of the complex. Anal. Calcd (found) for K[Fe$\mathbf{1}^{cyp}$(NO)]·DMF [$C_{24}H_{40}FeKN_6O_5$]: C, 49.06 (49.04); H, 6.86, (6.56); N, 14.30 (14.16). FTIR (Nujol, cm^{-1}), ν(NO) 1739 (s), 1712 (sh), ν(CO, DMF) 1681 (s), ν(CO, amide) 1596 (s), 1567 (s), 1560 (s); λ_{max} (DMF, ϵ, M^{-1} cm^{-1}), 836 (160), 514 (570), 378 (5200), 332 (4700); μ_{eff} (powder, 298 K) 4.32 μ_{BM}; μ_{eff} (DMSO-d_6, 298 °K) 4.01 μ_{BM}.

Potassium [(Tris(*N*-isopropylcarbamoylmethyl)aminato)(nitroso)]ferrate(III) (K[Fe1^{i}Pr(NO)]·DMF). The complex was synthesized following the procedure described for K[Fe$\mathbf{1}^{cyp}$(NO)]·DMF with 70% yield. Anal. Calcd (found) for K[Fe$\mathbf{1}^{i}$Pr(NO)]·DMF [$C_{18}H_{34}FeKN_6O_5$]: C, 42.43 (42.20); H, 6.73, (6.52); N, 16.49 (16.06). FTIR (Nujol, cm^{-1}), ν(NO) 1729 (s), 1712 (sh), ν(CO, DMF) 1679 (s), ν(CO, amide) 1594 (s), 1582 (s), 1559 (s); λ_{max} (DMF, ϵ, M^{-1} cm^{-1}), 840 (170), 512 (620), 372 (6700), 324 (6900); μ_{eff} (powder, 298 °K) 3.98 μ_{BM}; μ_{eff} (DMSO-d_6, 298 K) 4.03 μ_{BM}.

Potassium [(Tris(*N*-(3,5-dimethylphenyl)carbamoylmethyl)aminato)(nitroso)]ferrate(III) (K[Fe(1^{dmp})(NO)]). A solution of $H_3\mathbf{1}^{dmp}$ (0.290 g, 0.578 mmol) in 10 mL anhydrous DMF was treated with solid KH (0.070 g, 1.74 mmol) under an Ar atmosphere. After gas evolution ceased, solid $Fe(OAc)_2$ (0.101 g, 0.580 mmol) was added slowly. The resulting light yellow solution was stirred for 1 h and filtered to remove KOAc formed in the reaction. The filtrate was concentrated to 4 mL, and 5 mL of MeCN was added. The resultant solution was transferred to a Schlenk tube, and 15 mL (0.67 mmol) of NO was added by injecting from a gastight syringe. The solution's color changed rapidly to red brown. After stirring for 15 min, 40 mL of diethyl ether was added slowly to the reaction mixture. The complex K[Fe$\mathbf{1}^{dmp}$(NO)] was isolated as dark red crystalline solid (0.28 g, 80%) after 2 days. An analytically pure sample was prepared by recrystallizing the powder from DMF/diethyl ether. X-ray-quality crystals were grown by diffusing diethyl ether into DMF solution of the complex. Anal. Calcd (found) for K[Fe$\mathbf{1}^{dmp}$(NO)] [$C_{30}H_{33}FeKN_5O_4$]: C, 57.88 (57.35); H, 5.34 (4.74); N, 11.25 (10.95). FTIR (Nujol, cm^{-1}) ν(NO) 1750 (s); ν(CO) 1618 (s), 1611 (s), 1601 (s), 1582 (s); λ_{max} (DMF, ϵ, M^{-1} cm^{-1}), 783 (120), 508 (390), 357 (3200); μ_{eff} (powder, 298 K) 4.40 μ_{BM}; μ_{eff} (DMSO-d_6, 298 °K) 4.40 μ_{BM}.

Physical Methods. Elemental analyses were performed by Desert Analytics (Tucson, Arizona). All samples used for elemental analyses were dried under vacuum before shipment. The presence of solvates was corroborated by FTIR and ^{1}H NMR spectroscopy. Electronic spectra were recorded with a SLM-Aminco 3000 diode array spectrophotometer. ^{1}H NMR spectra were recorded either on Brüker DRX 400 MHz equipped with a SGI workstation or GE QE 300 MHz spectrometer. Chemical shifts are reported in ppm relative to an internal standard of TMS. FTIR spectra were recorded either on Mattson Sirius 100 (with an 4326 upgrade) or on ATI Mattson Genesis series FTIR spectrometer and are reported in wavenumbers. Fast atom bombardment mass spectra (FAB) were recorded on a Hewlett-Packard 5989 A spectrometer. Room-temperature magnetic susceptibility measurements of the solid samples were obtained using a magnetic susceptibility balance MSB-1 manufactured by Johnson Matthey. Solution magnetic moments were measured following Evan's method.[12] Diamagnetic corrections were taken from those reported by O'Connor.[13] X-band EPR spectra were recorded on a Bruker ESP 300 spectrometer equipped with an Oxford Instruments ESR 910 liquid helium cryostat. All spectra were obtained under nonsaturating conditions. The magnetic field was calibrated with an NMR gaussmeter and the microwave frequency was measured with a Hewlett-Packard 5352B Microwave Frequency Counter. Mössbauer spectra were obtained on a constant acceleration instrument and isomeric shifts are reported relative to an iron metal standard.

Cyclic voltammetric experiments were conducted using a BAS CV 50W (Bioanalytical Systems Inc., West Lafayette, IN) voltammetric analyzer. All experiments were done under argon at ambient temperature in solutions with 0.1 M tetrabutylammonium hexafluorophosphate at the supporting electrolyte. Anhydrous DMF was obtained from Burdick-Jackson Laboratory and used without further purification. Cyclic voltammograms (CV) were obtained using a three-electrode system consisting of a glassy-carbon working electrode, a platinum wire auxiliary electrode and a glass encased nonaqueous silver−silver nitrate reference electrode containing a Vycor plug to separate it from the bulk solution. A ferrocinium/ferrocene couple was used to monitor the reference electrode and was observed at 0.46 V with $\Delta E_p = 0.070$ V and $i_{pc} \cdot i_{pa}^{-1} \cong 1.0$ in DMF. IR compensation was achieved before each CV was recorded. Potentials are reported vs the saturated calomel couple. Controlled potential coulometry was performed with a PAR 175 digital coulometer using a system composed of a platinum mesh working electrode, a platinum mesh auxiliary electrode encased in a glass tube with supporting electrolyte solution and separated from the bulk solution by a medium porous glass frit, and the same silver−silver nitrate reference electrode used for the CV experiments.

Crystallographic Structural Determination. Crystal, data collection, and refinement parameters are given in Table 1. Suitable crystals for single-crystal X-ray diffraction were selected and mounted in

(12) (a) Evans, D. F. *J. Chem Soc.* **1959**, 2003. (b) Sur, S. K. *J. Magn. Reson.* **1989**, *82*, 169.
(13) O'Connor, C. J. *Prog. Inorg. Chem.* **1992**, 29, 203.

Table 1. Summary of Crystallographic Data and Parameters for $[Fe\mathbf{1}^{R}(NO)]^{-}$ Complexes

complex	K[Fe**1**^{iPr}(NO)]·DMF	K[Fe**1**^{cyp}(NO)]·DMF	K[Fe**1**^{dmp}(NO)]
molecular formula	$C_{18}H_{34}FeKN_6O_5$	$C_{24}H_{40}FeKN_6O_5$	$C_{30}H_{33}FeKN_5O_4$
fm	509.46	587.56	622.56
T (°C)	25	−100	−50
cryst syst	triclinic	triclinic	monoclinic
space group	$P\bar{1}$	$P\bar{1}$	$P2_1/n$
a (Å)	9.427(2)	14.363(5)	13.8253(2)
b (Å)	10.841(2)	10.929(8)	11.3653(2)
c (Å)	12.952(2)	9.517(3)	20.9166(3)
α (deg)	82.884(14)	82.77(4)	90
β (deg)	87.052(18)	97.20(3)	104.4450(10)
γ (deg)	83.993(15)	99.72(4)	90
Z	2	2	4
V (Å^3)	1305.2(4)	1453(1)	3182.70(9)
μ_{calc} (cm^{-1})	7.74	58.06	6.45
δ_{calc} (g/cm^3)	1.296	1.343	1.299
λ (Å)	0.710 73	1.541 78	0.710 73
R^b	0.0519	0.051	0.0284
$R_w{}^c$	0.1013	0.074	0.0930

[a] $R = [\sum|\Delta F|/\sum|F_o|]$. [b] $R_w = [\sum\omega(\Delta F)^2/\sum\omega F_o{}^2]^{1/2}$.

nitrogen-flushed, thin-walled glass capillaries. The data for K[Fe**1**^{i}Pr-(NO)]·DMF was collected on a Siemens P4 diffractometer, that for K[Fe**1**^{dmp}(NO)] was collected on a Siemens P4 diffractometer equipped with a SMART/CCD detector, and that for K[Fe**1**^{cyp}(NO)]·DMF was obtained using a Rigaku AFC5S diffractometer containing a 12 kW rotating anode generator.

No evidence of symmetry higher than triclinic was observed in either the photographic or the diffraction data for K[Fe**1**^{i}Pr(NO)]·DMF and K[Fe**1**^{cyp}(NO)]·DMF, and the systematic absences in the diffraction data are uniquely consistent for the reported space group for K[Fe**1**^{dmp}(NO)]. E statistics suggested the centrosymmetric space group, $P\bar{1}$, for K[Fe**1**^{i}Pr(NO)]·DMF and K[Fe**1**^{cyp}(NO)]·DMF, which yielded chemically reasonable and computationally stable results of refinement. The structures were solved by direct methods, completed by subsequent difference Fourier syntheses and refined by full-matrix least-squares procedures. A semiempirical ellipsoid absorption correction was applied to K[Fe**1**^{i}Pr(NO)]·DMF but was not necessary for K[Fe**1**^{cyp}(NO)]·DMF or K[Fe**1**^{i}Pr(NO)]·DMF because there was less than 10% variation in the integrated 41-scan intensity data. A molecule of DMF was located in the asymmetric units of K[Fe**1**^{i}Pr(NO)]·DMF and K[Fe**1**^{cyp}(NO)]·DMF. All non-hydrogen atoms were refined with anisotropic displacement parameters and hydrogen atoms were treated as idealized contributions. All software and sources of the scattering factors are contained in the SHELXTL (5.3) program library (G. Sheldrick, Siemens XRD, Madison, WI).

Results and Discussion

Synthesis and Characterization. In solution the $[Fe\mathbf{1}^{R}]^{-}$ complexes rapidly bind NO as indicated by the formation of intensely red-colored solutions (eq 1). The $[Fe\mathbf{1}^{R}(NO)]^{1-}$ complexes

$$\underset{\text{pale yellow}}{K[Fe\mathbf{1}^{R}]^{-}} \xrightarrow[DMF]{NO} \underset{\text{red-brown}}{K[Fe\mathbf{1}^{R}(NO)]^{-}} \qquad (1)$$

have similar electronic absorbance spectra that contain three visible bands at approximately 350, 500, and 800 nm (Figure 1, Table 4). Similar absorbance spectra have been observed for other non- heme $\{Fe-NO\}^7$ complexes.[6f] In the solid state, NO binding appears to be irreversible as no color changes were observed after placing the complexes under vaccum for several hours (>12 h). Fourier transform infrared spectra of all the complexes show strong peaks between 1710 and 1750 cm^{-1} which are assigned to the stretching frequecies of the coordinated nitrosyl ligands. These data agree with those reported for other

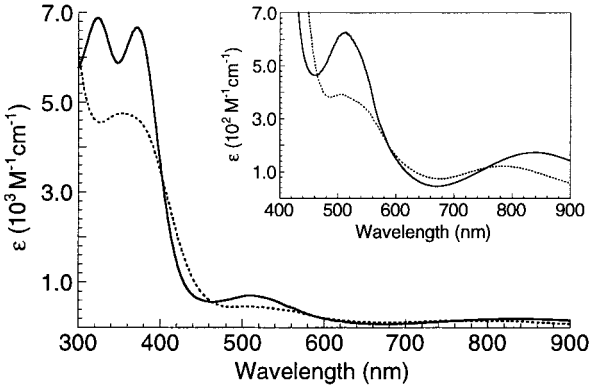

Figure 1. Electronic spectra of $[Fe\mathbf{1}^{i}Pr(NO)]^{1-}$ (−) and $[Fe\mathbf{1}^{dmp}(NO)]^{1-}$ (···) in DMF. Inset shows details between 400 and 900 nm.

Table 2. Selected Bond Distances and Angles for $[Fe\mathbf{1}^{R}(NO)]^{-}$ Complexes

distance (Å) or angle (deg)	$[Fe\mathbf{1}^{iPr}(NO)]^{-}$	$[Fe\mathbf{1}^{cyp}(NO)]^{-}$	$[Fe\mathbf{1}^{dmp}(NO)]^{-}$
Fe−N(1)	2.027(4)	2.032(4)	2.024(2)
Fe−N(2)	2.028(3)	2.020(4)	2.036(2)
Fe−N(3)	2.025(4)	2.027(4)	2.017(2)
Fe−N(4)	2.189(3)	2.184(4)	2.198(2)
Fe−N(5)	1.735(4)	1.737(4)	1.748(2)
N(5)−O(5)	1.122(5)	1.138(5)	1.146(3)
N(1)−Fe−N(2)	114.74(14)	115.9(2)	116.00(7)
N(2)−Fe−N(3)	115.5(2)	115.0(2)	115.32(7)
N(3)−Fe−N(1)	117.0(2)	116.2(2)	117.52(7)
N(4)−Fe−N(5)	179.2(2)	179.4(2)	175.47(2)
Fe−N(5)−O(5)	178.2(5)	172.7(4)	160.3(2)
d[Fe−N$_{amid}$][a]	0.424	0.428	0.395

[a] Displacement of Fe from the plane formed by N(1)−N(2)−N(3).

$\{Fe-NO\}^7$ complexes where the NO stretching frequency ranges from 1690 to 1840 cm^{-1}.[6,7]

Solid-State Structures. Single-crystal X-ray diffraction studies on the three $\{Fe-NO\}^7$ complexes confirms the coordination of an NO molecule to the iron resulting in an overall trigonal bipyramidal (TBP) coordination geometry. Selected distances and angles for structures of these complexes are shown in Table 2 and Figure 2 contains the thermal ellipsoid diagrams and space-filling representation of each complex. Additional structural parameters are provided in the Supporting Information.

The molecular structures of $[Fe\mathbf{1}^{i}Pr(NO)]^{-}$, $[Fe\mathbf{1}^{cyp}(NO)]^{-}$, and $[Fe\mathbf{1}^{dmp}(NO)]^{-}$ (Figure 2) show that the three amidate nitrogen donors from the tripodal ligands are arranged in the trigonal plane around the iron center. The trigonal bipyramidal coordination sphere is completed by the trans positioning of the apical N(4) donors of $[\mathbf{1}^{R}]^{3-}$ and nitrosyl nitrogens N(5). The average $N_{amid}-Fe-N_{amid}$ angle for the complexes are 115.74(1)° for $[Fe\mathbf{1}^{i}Pr(NO)]^{-}$, 115.7(1)° for $[Fe\mathbf{1}^{cyp}(NO)]^{-}$, and 116.28(4)° for $[Fe\mathbf{1}^{dmp}(NO)]^{-}$. These angles are lower from the 120° expected for trigonal bipyramidal geometry because the iron sits out of the trigonal plane (0.39−0.43 Å) toward N(5). The average $Fe-N_{amid}$ bond lengths for the three $[Fe\mathbf{1}^{R}(NO)]^{1-}$ complexes are virtually identical: 2.027(2) Å for $[Fe\mathbf{1}^{i}Pr(NO)]^{-}$, and 2.026(2) and 2.026(1) Å for $[Fe\mathbf{1}^{cyp}(NO)]^{-}$. Surprisingly, these bond distances are comparable to that observed in the $[Fe\mathbf{1}^{i}Pr]^{-}$ (2.027(2) Å), the Fe(II) precursor complex, which has a trigonal monopyramidal coordination geometry.[11b]

The spin state and oxidation state of metal ions often influence metal−ligand bond distances. For example, we have observed previously the shortening of average $Fe-N_{amid}$ bond length in low-spin $[Fe\mathbf{1}^{i}Pr(CO)]^{-}$ ($S = 1$) by 0.023 Å compared to high-

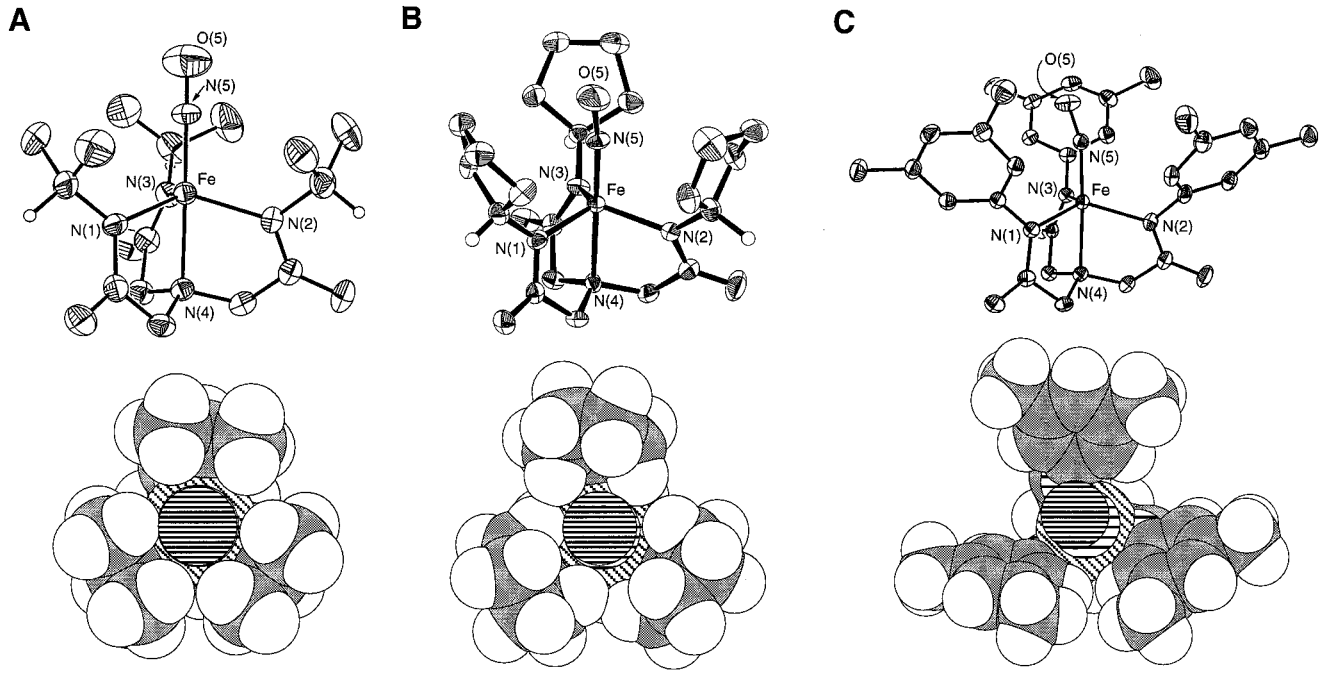

Figure 2. Thermal ellipsoid diagrams of [Fe**1**^{i}Pr(NO)]$^{-}$ (A, top), [Fe**1**^{cyp}(NO)]$^{-}$ (B, top), and [Fe**1**^{dmp}(NO)]$^{-}$ (C, top) and space-filling representations of each complex viewed down their respective pseudo 3-fold axis. The ellipsoids are drawn at the 30% probability level, and all non-methine hydrogens are removed for clarity.

spin [Fe**1**^{i}Pr]$^{-}$ ($S = 2$).[11b] This constrasts to the current results for the [Fe**1**^{R}(NO)]$^{-}$ complexes which have been formulated as $Fe^{3+}-NO^{-}$ species (vide infra). Thus no adjustment in the Fe−N bond distances was observed for this change in the iron center. A similar observation in six-coordinate {Fe−NO}^{7} complexes has been reported by Que and co-workers who saw no change in bond length for a change in oxidation state.[6f] They attribute factors other than oxidation state, such as strong metal−ligand interactions, that can counterbalance this effect and render bond lengths essentially unperturbed.

The most significant difference between the molecular structures of the [Fe**1**^{R}(NO)]$^{-}$ complexes are their Fe−N(5)−O(5) angles which relate to the size of the enclosing cavity. In [Fe**1**^{i}Pr(NO)]$^{-}$, which has a more restricted cavity with a diameter of ∼3 Å, a nearly linear Fe−N(5)−O(5) angle is observed (178.2(5)°). A larger and more flexible cavity (∼8 Å in diameter) which is formed by planar phenyl rings in [Fe**1**^{dmp}(NO)]$^{-}$ has a significantly smaller Fe−N(5)−O(5) angle of 160.3(2)°. This nonlinear angle lies within the range reported for most other non-heme {Fe−NO}^{7} complexes which lack restrictive cavities around the Fe−NO moiety. An additional complex, [Fe**1**^{cyp}(NO)]$^{-}$, has a cavity similar to that found in [Fe**1**^{i}Pr(NO)]$^{-}$ and a correspondingly similar Fe−N(5)−O(5) angle of 172.7(4)°. This relationship between cavity structure and Fe−N−O angle was also observed in the solid-state structure of [Fe**1**$^{S\text{-mbz}}$(NO)]$^{-}$.[10] The cavity surrounding the Fe−NO unit in [Fe**1**$^{S\text{-mbz}}$(NO)]$^{-}$ is flexible because the benzene ring of the methylbenzyl group can adopt different conformations. Crystallization of the potassium salt of [Fe**1**$^{S\text{-mbz}}$(NO)]$^{-}$ resulted in four crystallographically independent complexes in the asymmetric unit. These complexes differ by cavity size and their Fe−N−O angles. The smallest cavity has an Fe−N−O angle of 175.6(5)°, while an angle of 157.0(5)° is observed for the complex with the largest cavity.

Magnetization, EPR, and Mössbauer Spectroscopy. The room-temperature magnetic moments of the nitrosyl complexes in solution and the solid state are given in Table 3. The values range from 3.98 to 4.40 μ_{BM} and are close to the spin-only value for an $S = {}^{3}/_{2}$ complex of 3.87 μ_{BM}.

Table 3. Magnetic, EPR, and Mössbauer Parameters for [Fe**1**^{R}(NO)]$^{-}$ Complexes

complex	$\mu_{eff}(\mu_{BM})$	E/D[c]	$\sigma_{E/D}$	σ_B (mT)	δ (mm/s)[d]	ΔE_q (mm/s)[d]
[Fe**1**^{iPr}(NO)]$^{-}$	3.98,[a] 4.03[b]	0.062	0.025	7.8	0.427	1.294
[Fe**1**^{cyp}(NO)]$^{-}$	4.32,[a] 4.01[b]	0.072	0.024	5.6	0.412	1.336
[Fe**1**^{dmp}(NO)]$^{-}$	4.40,[a] 4.40[b]	0.090	0.020	4.1	0.430[e]	1.331[e]

[a] Powdered sample. [b] DMF solution, using the Evan's method. [c] All simulations used $\mathbf{g}_e = 2.00, 2.00$, and 2.01 for eq 2. [d] Data recorded at 4.2 K, 0.45 kG. [e] At 195 K, $\delta = 0.365$ mm/s, $\Delta E_q = 1.330$ mm/s.

Magnetic moments larger than the spin-only value may be due either to an orbital contribution to the spin-only moment or to population of an excited spin state. However, the EPR data (vide infra) allow an orbital contribution to the spin-only moment of no greater than 1%. Some other $S = {}^{3}/_{2}$ {Fe−NO}^{7} complexes also display magnetic moments which are higher than the spin-only value[7c] by comparable amounts.

The frozen solution EPR spectra of the three nitrosyl complexes, shown in Figure 3, are typical of slightly rhombic $S = {}^{3}/_{2}$ signals where $g_x \approx g_y \approx 4$ and $g_z \approx 2$. The spectra can be described with the standard spin Hamiltonian

$$H = \beta_e \mathbf{B}\cdot\mathbf{g}_e\cdot\mathbf{S} + D\left[(S_z^2 - {}^{5}/_{4}) + \frac{E}{D}(S_x^2 - S_y^2)\right] \qquad (2)$$

in which D and E are the axial and rhombic zero field splitting parameters, respectively. The temperature dependence of the signals from all three complexes indicate that all signals arise from a ground $|\pm{}^{1}/_{2}>$ doublet with $D > 0$. No significant features are observed from the excited $|\pm{}^{3}/_{2}>$ doublet at higher temperatures. Simulations of the signals were calculated from eq 2 using a line shape model which allows for a Gaussian distribution $\sigma_{E/D}$ in the rhombic parameter, and a spin-packet line width σ_B for unresolved hyperfine broadening. The simulations shown in Figure 3 (dashed lines) are least-squares fits

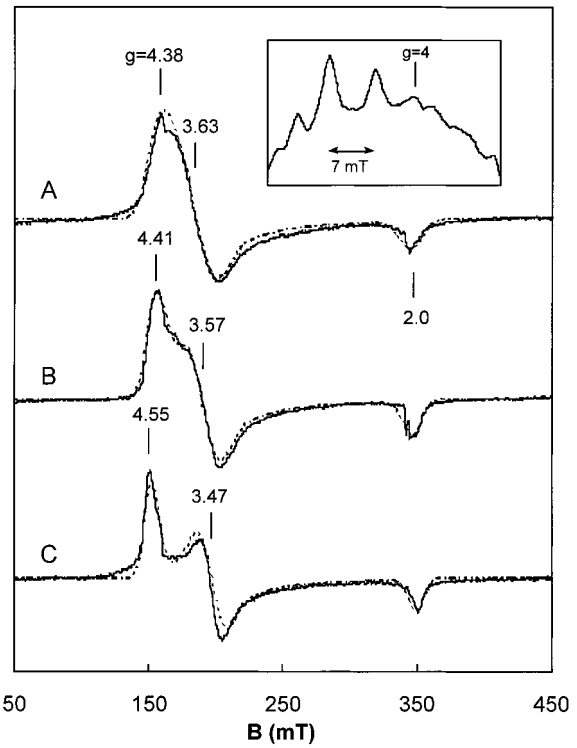

Figure 3. EPR spectra (−) and simulations (···) of frozen DMF solutions with nominal concentrations of 1 mM [Fe**1**^{i}Pr(NO)]$^{-}$ (A), [Fe**1**^{cyp}(NO)]$^{-}$ (B), and [Fe**1**^{dmp}(NO)]$^{-}$ (C). Instrumental parameters: 12 K; microwaves, 0.2 mW at 9.62 GHz; 1 mT modulation at 100 kHz. The simulation parameters can be found in Table 3. The inset shows the EPR spectrum of [Fe**1**^{i}Pr(NO)]$^{-}$ with instrumental parameters as above except 0.3 mT modulation.

derived from variation of the parameters E/D, $\sigma_{E/D}$, and σ_B. The best-fit parameters are given in Table 3. Both line width parameters are required to give reasonably good fits.

The signal line widths are dominated by partially resolved hyperfine splittings from the nitrogen ligands which results in some simulation mismatch. The [Fe**1**^{i}Pr(NO)]$^{-}$ complex shows additional features at $g \approx 4$ as shown in the inset of Figure 3. These features do not have regular spacing, probably due to multiple overlapping hyperfine patterns from the amide, amine, and nitrosyl nitrogens. The nitrosyl ligand, however, probably does not contribute significantly to the hyperfine pattern due to pairing of the nitrosyl electron with metal orbitals.[14]

Mössbauer spectra of the nitrosyl complexes exhibit simple quadrupole doublets at both low and high temperatures. The isomer shifts at 4.2 K, ranging from $\delta = 0.41-0.43$ mm/s, and the quadrupole splittings, ranging from $\Delta E_q = 1.29-1.33$ mm/s (Table 3), most closely match typical values of high spin ferric complexes. Although the isomer shift is also in the appropriate range for an Fe(II) $S = 1$ complex, data from the CO adducts of the four-coordinate iron complexes with the [**1**^{cyp}]$^{3-}$ and [**1**^{i}Pr]$^{3-}$ ligands which have an $S = 1$ configuration, have a much smaller isomer shift of $\delta = 0.26$ mm/s.[11b] Thus, the iron nuclei of the nitrosyl complexes are significantly more shielded from s electron density than that of the CO adducts, corroborating a high spin Fe(III) electronic configuration in the NO adducts, rather that an S = 1 configuration. At 195 K the measured isomer shift of K[Fe**1**^{dmp}(NO)] is slightly reduced as expected due to the second-order Doppler shift,[15] while the quadrupole splitting remains unchanged. High-spin Fe(III) complexes tend to have slow electronic relaxation times and thus give a six line magnetic spectrum in low magnetic fields. The Fe−NO complexes of this work, however, show only quadruple doublets in low magnetic field at 4.2 K, indicating fast electronic relaxation in the powder samples. Solution samples at high concentration (80 mM) in CH_3CN showed the same isomer shifts and quadruple splittings as the powder samples, but increased line widths, presumably due to slower relaxation in solution which results in a small residual magnetic moment. The EPR signals at lower concentration (∼1 mM) also show fast electronic relaxation as the signals are not saturable at 2 K and microwave powers of 200 mW.

Previously characterized {Fe−NO}^{7} complexes have been observed in spin states of either $S = {}^1/_2$[16,17] or $S = {}^3/_2$[6c−f] or to undergo a temperature-dependent transition between these two spin states.[7a,b] These complexes all have either octahedral or square pyramidal geometries. For iron porphyrin complexes, binding NO results in low spin complexes and may be approximated as $Fe^{2+}-NO^0$.[17] The non-heme NO complexes have been characterized as high-spin Fe(III) ($S = {}^5/_2$) exchange coupled to NO^- ($S = 1$) to give an antiferromagnetic ground spin state of $S = {}^3/_2$.[14] The lower coordination number of the trigonal bipyramidal {Fe−NO}^{7} complexes described here produces a smaller ligand field splitting as compared to the more common six-coordinate iron-nitrosyl species. Nevertheless trigonal bipyramidal iron complexes with [**1**^{R}]$^{3-}$ ligands can undergo spin state transitions as has been observed [Fe**1**^{i}Pr(CO)]$^{-}$,[11b] thus, we must consider a variety of electronic models. The spin states of the [Fe**1**^{R}(NO)]$^{-}$ complexes studied here have been examined using room-temperature magnetic susceptibility, EPR, and Mössbauer spectroscopy. This information can be used to determine the oxidation state of the metal and the nitrosyl ligands as well as the electronic configurations of the complexes.

Four conceivable electronic structures could describe a trigonal bipyramidal $S = {}^3/_2$ {Fe−NO}^{7} complex. These are [Fe^{3+} d^5 HS ($S = {}^5/_2$)−NO^- ($S = 1$)][18] and [Fe^{2+} d^6 HS ($S = 2$)−NO^0 ($S = {}^1/_2$)][19] both antiferromagnetically coupled; [Fe^+ d^7 HS ($S = {}^3/_2$)−NO^+ ($S = 0$)];[20] and [Fe^{2+} d^6 LS ($S = 1$)−NO^0 ($S = {}^1/_2$)], ferromagnetically coupled. These possible configurations, differing in the oxidations states of the iron and the nitrosyl ligand can be distinguished with Mössbauer spectroscopy. The small isomer shifts and quadrupole splitting of the [Fe**1**^{R}(NO)] complexes indicate that the iron is in the high spin Fe(III) electronic configuration Thus, for the trigonal bipyramidal complexes considered here, only the Fe^{3+} d^5 HS ($S = {}^5/_2$)−NO^- ($S = 1$)] configuration agrees with the magnetic susceptibility, EPR and Mössbauer spectroscopy. The iron of the four-coordinate starting material has been oxidized by the NO ligand to give a system which can be formally described

(14) Brown, C. A.; Pavlosky, M. A.; Westre, T. E.; Zhang, Y.; Hedman, B.; Hodgson, K. O.; Solomon, E. I. *J. Am. Chem. Soc.* **1995**, *117*, 715.
(15) Lang, G. *Q. Rev. Biophys.* **1970**, *3*, 1.
(16) (a) Karlin, K. D.; Rabinowitz, H. N.; Lewis, D. L.; Lippard, S. J. *Inorg. Chem.* **1977**, *16*, 3292. (b) Berno, P.; Floriani, C.; Chiesi-Villa, A.; Guastini, C. *J. Chem. Soc., Dalton Trans.* **1988**, 1409. (c) Qian, L.; Singh, P.; Ro, H.; Hatfield, W. E. *Inorg. Chem.* **1990**, *29*, 761.
(17) (a) Scheidt, W. R.; Frisse, M. E. *J. Am. Chem. Soc.* **1975**, *97*, 17. (b) Scheidt, W. R.; Piciulo, P. *J. Am. Chem. Soc.* **1976**, *98*, 1913. (c) Scheidt, W. R.; Brinegar, A. C.; Ferro, E. B.; Kirner, J. F. *J. Am. Chem. Soc.* **1977**, *99*, 7315. (d) Scheidt, W. R.; Lee, Y. J.; Hatano, K. *J. Am. Chem. Soc.* **1984**, *106*, 3191. (e) Nasri, H.; Haller, K. J.; Wang, Y.; Huynh, B. H. and Scheidt, W. R. *Inorg. Chem.* **1992**, *31*, 3459.
(18) Zhang, Y.; Pavosky, M. A.; Brown, C. A.; Westre, T. E.; Hedman, B.; Hodgson, K. O.; Solomon, E. I. *J. Am. Chem. Soc.* **1992**, *114*, 9189.
(19) Salerno, J. C.; Siedow, J. N. *Biochim. Biophys. Acta* **1979**, *579*, 246.
(20) Wells, F. V.; McCann, S. W.; Wickman, H. H.; Kessel, S. L.; Hendrickson, D. N.; Feltham, R. D. *Inorg. Chem.* **1982**, *21*, 2306.

Table 4. Electronic Spectra[a] and Cyclic Voltammetric[b] Data for $[Fe\mathbf{1}^{R}(NO)]^{-}$ Complexes

complex	λ_{max}, nm (ϵ, M^{-1} cm^{-1})	oxidation $E_{1/2}$, V (ΔE_p, mV)	reduction $E_{1/2}$, V (ΔE_p, mV)
$[Fe\mathbf{1}^{iPr}(NO)]^{-}$	324 (6900), 372 (7600), 512 (620), 840 (170)	0.56 (65)	−1.57 (105)
$[Fe\mathbf{1}^{cyp}(NO)]^{-}$	332 (4700), 378 (5200), 514 (570), 836 (160)	0.55 (60)	−1.60 (76)
$[Fe\mathbf{1}^{dmp}(NO)]^{-}$	357 (3200), 508 (390), 783 (120)	0.61 (65)	−1.48 (110)

[a] Spectral measurements of DMF solution in the range 400−900 nm were made at ca. 10^{-3} M and for the 300−500 nm region were made at ca. 10^{-4} M. [b] Supporting electrolyte $[NBu^{n}_4]BF_4$ (0.15 M); all potentials are referenced to the SCE; $E_{1/2} = 0.5\ (E_{pc} + E_{pa})$ where E_{pc} and E_{pa} are the cathodic and anodic peak potentials, respectively; scan rate of 100 mV s^{-1} at a glassy carbon electrode.

as an NO^- ligand bound to Fe(III). The $S = {}^5/_2$ iron is antiferromagnetically coupled to the $S = 1$ NO^- ligand to give an $S = {}^3/_2$ system, which has also been found by Solomon and co-workers[14] to best describe the octahedral $S = {}^3/_2$ complexes, Fe(EDTA)(NO) and $Fe(Me_3TACN)(NO)(N_3)_2$.

In the literature much emphasis has been placed on the binding angle of the nitrosyl ligand to metal centers and the effect on the Fe−NO π-bonding.[7a,21] A bent NO is expected to lower the symmetry of the complex from axial, and thus increase the rhombic parameter *E/D* in EPR data. The value of E/D from Table 3 does follow this trend with the binding angle of the NO ligand, and agrees with the solid state molecular structures discussed previously. No significant differences between the bent and linearly bound NO complexes are observed from the Mössbauer data. Similarly, in studies of many other nitrosyl complexes, no correlation has been observed between the binding angle of the NO ligand and the N−O stretching frequency.[7c]

The simulations in Figure 3 are derived from eq 2 and require $\mathbf{g}_e = 2.00(1)$. Since the $\mathbf{g}_e$ values differ from the spin-only value by no more than 1%, the increase observed in the magnetic moment above the spin-only value cannot be due solely to an orbital contribution. Alternatively, the antiferromagnetic coupling between the $S = {}^5/_2$ Fe^{3+} and $S = 1$ NO^- will give excited spin manifolds of $S = {}^5/_2$ and ${}^7/_2$. Population of the $S = {}^5/_2$ state at room temperature would cause an increase in the effective magnetic moment. We have looked carefully for an excited $S = {}^5/_2$ signal in the EPR spectra up to 225 K. No such additional signals were observed to grow in, and the ground state signal remains clearly visible without a detectable decrease in its population. The origin of the deviation in the room temperature magnetic moments are currently unclear and will be resolved in later studies.

Electrochemistry. Cyclic voltammetry of the three complexes was performed in DMF with a glassy carbon electrode and the results are summarized in Table 4. All the complexes undergoes almost identical reversible oxidation ($\Delta E_p \sim 60$ mV) and quasi-reversible (ΔE_p range from 80 to 100 mV) reduction at the electrode surface (see Figure 4 for $[Fe\mathbf{1}^{cyp}(NO)]^-$). This observed small differences in the potentials for both redox processes between the three $\{Fe-NO\}^7$ complexes suggest that the donor abilities of the three tripodal ligands are nearly equivalent. Controlled potential coulometry (CPC) on $[Fe\mathbf{1}^{i}Pr(NO)]^-$ was used to explore the accessibility of oxidized products, such as $\{Fe-NO\}^6$ species. At a potential of 340 mv vs Ag/Ag^+, CPC experiments measured 1 e^-/mol of $[Fe\mathbf{1}^{i}Pr(NO)]^-$, which agrees

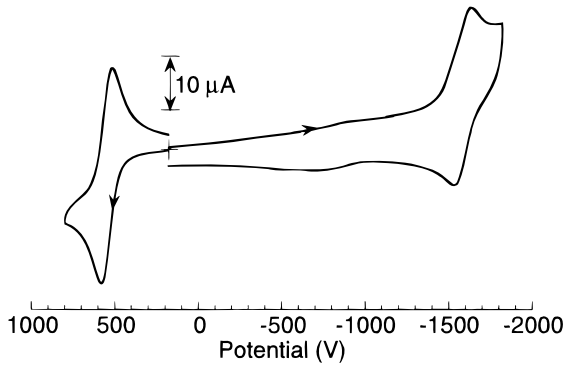

Figure 4. Cyclic voltammogram of $[Fe\mathbf{1}^{cyp}(NO)]^{1-}$ in DMF. Conditions: concentration, 1.64 mM; working electrode, glassy carbon; scan rate, 100 mVs^{-1}.

with the assignment of a one-electron oxidation of $[Fe\mathbf{1}^{i}Pr(NO)]^-$. Upon completion of the coulometric oxidation of $[Fe\mathbf{1}^{i}Pr(NO)]^-$, a deep red solution was generated which faded to a pale brown color within minutes. Cyclic voltammetry of this brown solution shows that only 40% of $[Fe\mathbf{1}^{i}Pr(NO)]^-$ is present. These cyclic voltammetric properties diminish further with time, indicating the instability of the oxidized $[Fe\mathbf{1}^{i}Pr(NO)]$ species generated in solution. Attempts to isolate the oxidized species were unsuccessful.[22]

Summary. We have demonstrated that the cavity structure around an Fe−NO unit affects its angle. Restricted cavities of smaller diameter yield nearly linear Fe−N−O angles as shown by the solid-state molecular structure of $[Fe\mathbf{1}^{i}Pr(NO)]^-$. Larger and potentially more flexible cavities yield smaller Fe−N−O angles of ∼160° as seen in $[Fe\mathbf{1}^{dmp}(NO)]^-$. EPR data of frozen solutions corroborate the results found in the solid state.

The Fe−NO angular results obtained here agree with those reported for other non-heme $\{Fe-NO\}^7$ complexes having $S = {}^3/_2$ ground states. Most of the previously characterized complexes that are either square pyramidal or six-coordinate have relatively unrestricted NO binding sites with Fe−N−O angles that range from 147 to 159°.[7] $[Fe(TMC)(NO)](BF_4)_2$ and an isomer of $[Fe\mathbf{1}^{S\text{-}mbz}(NO)]^-$ are the only other complexes with nearly linear Fe−N−O angles reported in the literature.[6a,10] Both complexes have restricted cavities; the former by four nearby methyl groups, the latter by *S*-benzylmethyl groups. Although an example of a trigonal bipyramidal $\{Fe-NO\}^7$ complex has been reported,[10] $[Fe\mathbf{1}^{R}(NO)]^-$ is the first series of related complexes that has allowed the examination of the magnetic and structural properties of this class of compounds.

Acknowledgment is made to the NIH (Grants GM50781 to A.S.B. and GM49970 to M.P.H), NSF for their support of the purchase of the CCD-based diffractometer at the University of Delaware (Grant CHE-9628768), and Professor E. Münck for use of his Mössbauer spectrometer.

Supporting Information Available: Tables of X-ray structural data for $K[Fe\mathbf{1}^{i}Pr(NO)]\cdot DMF$, $K[Fe\mathbf{1}^{cyp}(NO)]\cdot DMF$ and $K[Fe\mathbf{1}^{dmp}(NO)]$ (30 pages). This material is available free of charge via the Internet at http://pubs.acs.org.

IC990070A

(21) Hoffmann, R.; Chen, M. M. L.; Elian, M.; Rossi, A. R.; Mingos, D. M. P. *Inorg. Chem.* **1974**, *13*, 2666.

(22) An example of a non-heme $\{Fe-NO\}^6$ complex has recently been reported that models the inactive form of nitrile hydratase: Schweitzer, D.; Ellison, J. J.; Shoner, S. C.; Lovell, S.; Kovacs, J. A. *J. Am. Chem. Soc.* **1998**, *120*, 10996.